Configurable Multi-Port Memory Architecture for High-Speed Data Communication

Narendra Singh Dhakad D and Santosh Kumar Vishvakarma

Indian Institute of Technology Indore, India

Abstract—Memory management is necessary with the increasing number of multi-connected AI devices and data bandwidth issues. For this purpose, high-speed multi-port memory is used. The traditional multi-port memory solutions are hard-bounded to a fixed number of ports for read or write operations. In this work, we proposed a pseudo-quad-port memory architecture. Here, ports can be configured (1-port, 2-port, 3-port, 4-port) for all possible combinations of read/write operations for the 6T static random access memory (SRAM) memory array, which improves the speed and reduces the bandwidth for data transfer. The proposed architecture improves the bandwidth of data transfer by $4\times$. The proposed solution provides $1.3\times$ and $2\times$ area efficiency as compared to dual-port 8T and quad-port 12T SRAM. All the design and performance analyses are done using 65nm CMOS technology.

Index Terms—Multi-port memory, memory addressing, high-bandwidth memory

I. INTRODUCTION

Emory plays a crucial role in electronic systems. With the advancement of edge AI devices, efficient memory management is essential. Due to their complex computational needs, graphic, audio, and video processing require heterogeneous and multi-core processors. Multi-port memories have become vital for CPUs since multi-core processors demand significant data transfer capabilities. For edge AI applications such as smartwatches and autonomous cars, which receive or transfer data from various sources, reconfigurable multiport memories are necessary for fast and efficient design. However, multi-port memories come with increased area and leakage costs. Traditionally, dual-port SRAMs use an 8T SRAM bitcell, which has a high area and leakage and faces contention issues when read word line (RWL) and write word line (WWL) is selected for the same bitcell. The write driver can disturb stored data by driving the write bitline. Similar problems can occur in most conventional dual-port memories, such as 8T, 10T, and 12T configurations. Additionally, this memory architecture can only function as a two-port memory, with one port fixed for reading and the other for writing. [1]-[3].

This paper presents a wrapper circuit that transforms a conventional single-port 6T SRAM macro into a multi-port configuration. The architecture offers flexibility, allowing it to be configured for 1-port, 2-port, 3-port, or 4-port operations. The proposed approach avoids contention issues by accessing the cell sequentially, enhancing read and write robustness. Additionally, the ports can be configured for various combinations of read and write operations, such as 1-read/3-write, 2-read/2-write, 3-read/1-write, or all read/write ports.

TABLE I: AVAILABLE MULTI-PORT ARCHITECTURES

Parameters	1R1W [3]	2R2W [4]	8R1W [5]	5R1W [6]	6R2W [7]	6R6W [8]	4R1W [9]	multi-port [10]
Bitcell	8T	12T	20T	16T	24T	16T	-	DRAM
#N Ports	2	4	9	6	8	12	5	N
Ports	Fixed	Fixed	Fixed	Fixed	Fixed	Fixed	Configurable	Configurable
Approach	Bitcell	Bitcell	Bitcell	Bitcell	Bitcell	Bitcell	Algorithm	Coding

Utilizing 6T SRAM bit cells increases the memory array density, improving area efficiency. Integrating a wrapper for latches and multiplexers around a regular single-port SRAM enables pseudo-multi-port operation.

A simpler way to add multiple ports is to modify the memory cell with additional wordlines and bitlines. Many works [1]–[3] have been proposed for dual port work, where one port is used for read and another for write operation and [4]–[8] presented multi-port memory designs. However, these ports are hard-bounded and can not change operations once fabricated. Also, such dual-port SRAMs use a higher transistor SRAM bitcell, which increases the area and leakage and also suffers from contention issues.

An algorithmic multi-port memory configuration is presented in [9], which schedules multi-port memory instructions in the framework by extracting parallelism from the algorithm trace. Similarly, a coding-based solution is proposed in [10]. These approaches are effective for field programmable gate arrays (FPGAs) but cannot be deployed for memory chip design.

2R2W [4] proposed a four-port 12T memory cell that can perform two red and two write operations. However, it has an area overhead of twice as compared to conventional 6T SRAM-based memory. Also, multiple ports at the cell level include additional routing wires, increasing the memory macro's area and delay.

A pseudo-multi-port SRAM circuit was introduced in [11]. The design is explicitly tailored for image processing tasks in display drivers. Unlike traditional SRAM designs, this circuit incorporates multiple ports in a pseudo manner. The pseudo-multi-port SRAM circuit introduces additional complexity to the memory design, requiring careful implementation and validation to ensure reliable operation. This complexity also increases the manufacturing cost, requiring additional routing for additional ports and huge area overhead. Table I shows the cumulative study of different multi-port memory architectures in the literature.

The major advantages of the proposed work are as follows:

 A wrapper circuit is proposed to configure single-port SRAM into multi-port memory.

- The architecture can configure the SRAM macro as either 1-port, 2-port, 3-port or 4-port memory.
- The ports can be used as any combination of read and write operations.
- The solution enhances the memory access speed by $4\times$.
- The architecture provides an area-efficient solution to design multi-port memory architecture compared to other available work.

II. PROPOSED MULTI-PORT SRAM MEMORY ARCHITECTURE

To address the issues of area overhead and circuit complexity, we have proposed a wrapper for conventional memory architecture, which uses the conventional single-port memory architecture for configurable read/write operations from multiple ports. Fig. 1 shows the proposed multi-port architecture in which a wrapper circuit controls an SRAM macro. The wrapper circuit includes multiple input/output ports, a priority encoder, a clock generator, a finite state machine (FSM) and selection circuitry (multiplexer, decoder). Fig. 1 shows an example of 4 ports, which can be configured for both read and write operations. Each port has a port enable signal $(port_en)$, read/write enable signal (w/rb), address line (addr), and data line (w_data) . The ports are controlled by an external clock (CLK). Let us understand the functionality of each block.

A. Different Blocks of Architecture

- 1) Multiple Ports: The architecture shown in Fig. 1 has four ports. Each port has one enable signal $port_en$. By activating the $port_en$ signal, any ports can be enabled. Based on the number of ports enabled, the architecture can be called as 1-port, 2-port, 3-port or 4-port memory. Accordingly, the N ports en block gives the enabled port count (B1B0) to the elk_gen block, which later generates the internal clocks to switch the input/output of/from the ports. Once the port is enabled, it must be configured for read or write operation by selecting the w/rb signal. For w/rb = 1, the port will perform the write operation; for w/rb = 0, the port will perform the read operation. The address is given through the addr signal for read or write operations. Signal w_data is used to provide the data to be written in the memory if w/rb = 1.
- 2) SRAM Macro: SRAM macro consists of a 6T SRAM-based memory array. Whose memory cells are selected by the enable ports through the multiplexer. Based on the port enabled $(port_en)$ and the address (addr) given through the selected port, data is written or read (w/rb) from the respective cell.
- 3) Priority Encoder: A priority encoder is used to assign priority to the enabled ports. Let us assume all four ports are enabled; priority can be given to ports, like A>B>C>D, based on the requirement. Based on the priority signal of the port, the FSM generates a selection signal for the MUX and transits to the next state according to the current state to transfer the data to/from the port to SRAM macro. This avoids contention issues, enhancing the responsiveness and reliability of the system.

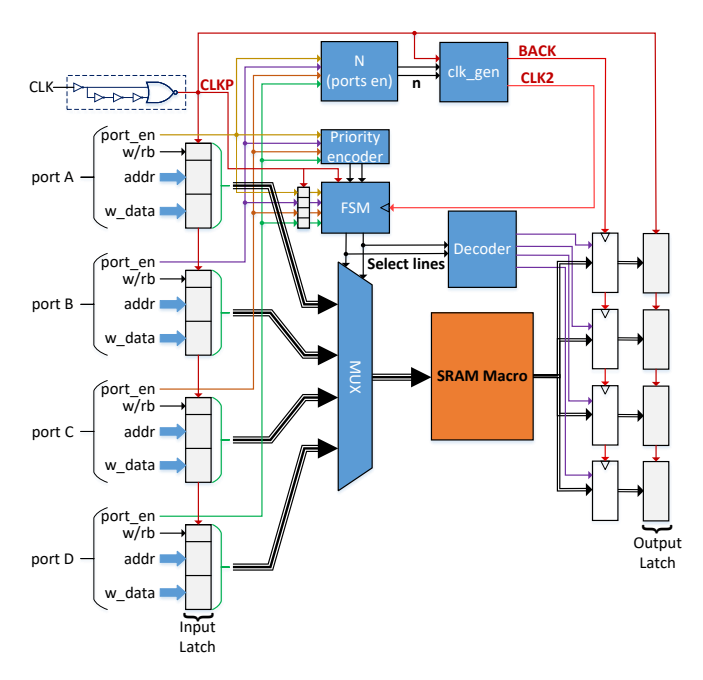


Fig. 1: Proposed quad-port memory architecture. Here, SRAM macro is the conventional 6T SRAM macro

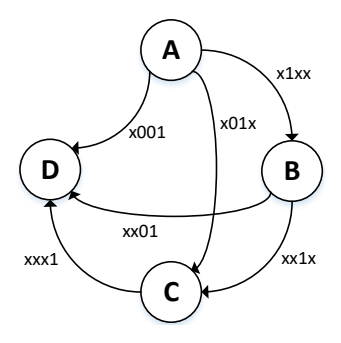


Fig. 2: State diagram shows the change of states of FSM. Here, it has been considered that the priority of the ports is A > B > C > D. So the transition of ports starts from port A and goes till port D, later resets to port A.

- 4) Finite State Machine: Finite State Machine (FSM) changes the state based on port priority. Fig. 2 shows the example of the state diagram of the FSM, where the state changes from one port to another. Transitioning between predefined states in response to inputs from multiple ports, each assigned a specific priority. When simultaneous inputs are received, the FSM evaluates the priority of each port, using priority mapping to determine the highest-priority input. The transition function then dictates the next state based on the current state, and this prioritizes input, ensuring that the most critical port connects with the SRAM macro. FSM ensures a controlled and deterministic state transition mechanism, enhancing the system's responsiveness and reliability in scenarios where multiple inputs compete for attention.
- 5) Clock Generator: The clock generator is the main block of the complete wrapper, which configures the memory architecture in different port memory modes. Fig. 3 shows the internal view of the clock generator block. The main function

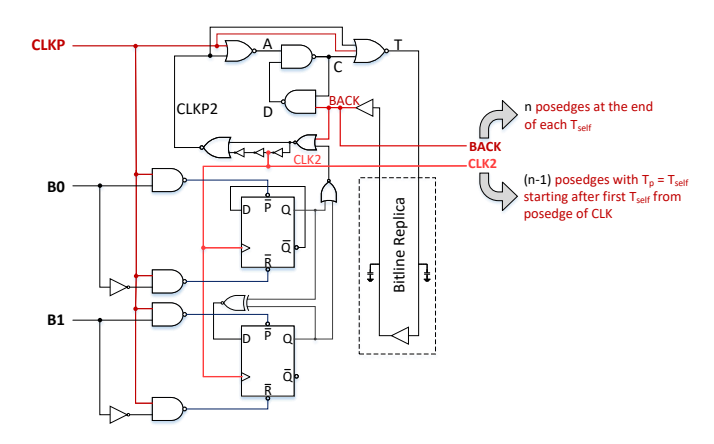


Fig. 3: Block diagram of clock generator. Here, simulation is shown for 4 cases

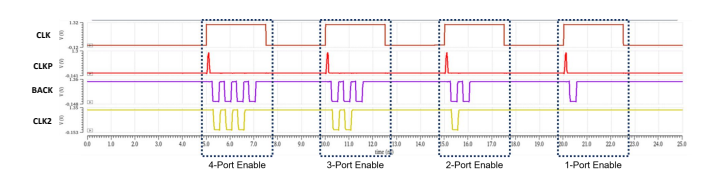


Fig. 4: Simulation waveform for the clock generator. Here, simulation has been configured to 4-port, 3-port, 2-port, and 1-port memory architecture in different clocks.

of the clock generator is to generate the BACK and CLK2 pulses to switch the states of FSM and initialize the highest priority port after each clock CLK. The clock generator divides the external clock CLK into multiple internal clocks based on the number of ports enabled. Fig. 4 shows the simulation waveform of the clock generator. Here, the external clock CLK is applied at 250MHz. The signal CLKP generates the spikes at the positive edge of each clock. Based on the number of ports enabled, it divides the CLK and generates BACK and CLK2 signals. BACK signal includes N pulses, and CLK2 generates N-1 pulses for single CLK duration. The clock generator takes the number of port-enabled counts as input B1 & B0 $(00 \Rightarrow 1\text{-port}, 01 \Rightarrow 2\text{-port}, 10 \Rightarrow 3\text{-port}, 11 \Rightarrow 4\text{-port})$ and accordingly generates BACK and CLK2 pulses.

B. Functionality of the Architecture

The performance evolved around how data is received, and based on that, the states of the FSM changed. Let us consider all four ports are enabled, which means the architecture works as a quad-port. The inputs at ports A, B, C, and D get latched using CLKP as an input signal and select lines of the multiplexer to get initialized to port A. Output register corresponding to port A also gets enabled to latch the read out triggered by $posedge\ of\ BACK$ temporarily occurs at the end of the operation cycle. In the next operation cycle, select lines change to port B, and the output register corresponding to port B gets enabled, and this process continues. As four ports are enabled, there in three (N-1) transitions in the state of select lines (CLK2) for that we get four (N) positive edges

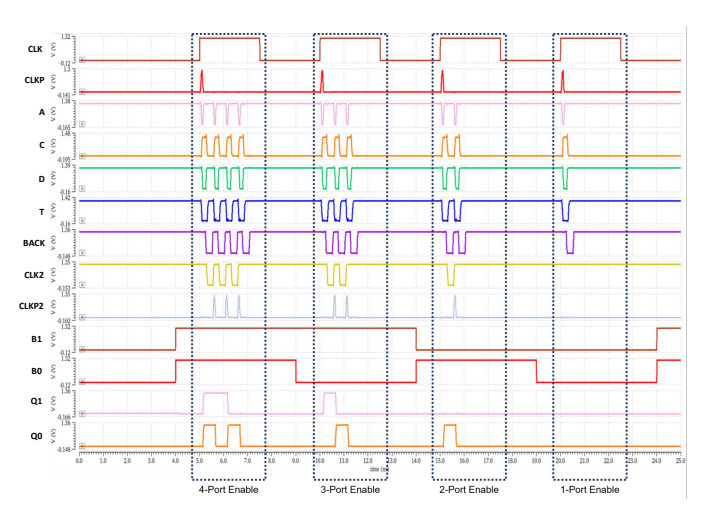


Fig. 5: Simulation waveform of the overall functionality of the proposed quad-port memory architecture. Here, simulation has been configured to 4-port, 3-port, 2-port, and 1-port memory architecture in different clocks.

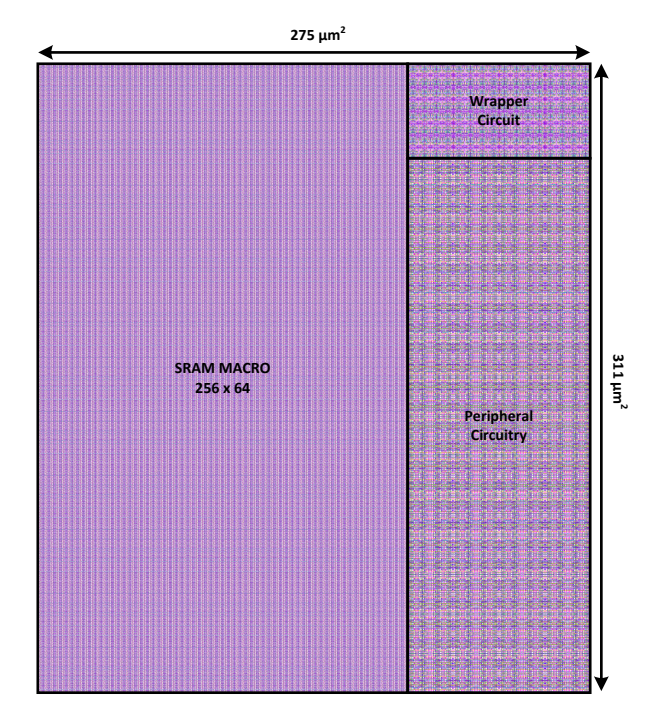


Fig. 6: Layout of the overall architecture of the proposed quadport memory architecture.

in BACK signal. To get the (N-1) transitions in the select lines of the multiplexer, we require a signal CLK2, which is generated by a clock generator. The FSM changes its state at every $posedge\ of\ CLK2$ based on the input $(port_en)$ signals. The state of FSM returns back to the enabled port with the highest priority (A>B>C>D) at every $posedge\ of\ CLK$ by the asynchronous loading output of the priority encoder. At the next cycle of CLK, the data in the output registers got latched to the read ports.

TABLE II: PERFORMANCE COMPARISON

Parameters	1R1W [3]	2R2W [4]	8R1W [5]	5R1W [6]	6R2W [7]	6R6W [8]	Proposed
Technology	14nm	6nm	40nm	90nm	32nm	7nm	65nm
Bitcell	8T	12T	20T	16T	24T	16T	6T
Bitcell Area*	1.3×	2×	3.3×	2.6×	4×	2.6×	1×
#N Ports	2	4	9	6	8	12	4
Ports	Fixed	Fixed	Fixed	Fixed	Fixed	Fixed	Configurable
Freq. (Memory Access)	2.33 GHz	-	-	1.5 GHz	250 MHz	2.59 GHz	1 GHz
Supply Voltage	1.1	0.9	_	_	0.4	0.9	1.2
Array Size	72Kb	16Kb	_	4Kb	4Kb	4Kb	16Kb
Area (mm ²)	-	-	-	-	0.05	0.08	0.085

*Area has been scaled with respect to 6T SRAM cell for fair comparison among different technology nodes

III. PERFORMANCE ANALYSIS

The proposed architecture is designed with a 65nm CMOS technology node using Cadence Virtuoso and evaluated using post-layout simulations. Fig. 6 shows the layout of the overall architecture shown in Fig. 1. Here, the wrapper circuit increases the area overhead by only 8% for an SRAM macro of 16Kb. This is minimal compared to the area overhead due to the bitcell modification for 8T/12T/20T, etc., to add the additional ports. Fig. 5 shows the simulation waveform for a quad-port-enabled system. Simulation waveforms show all the internal signals of the clock generator. Here, for each clock of CLK, the architecture is scheduled to work as 4-port, 3-port, 2-port, and 1-port, respectively. Here, it can be observed that in a single clock period of external clock CLK, the BACKsignal generates the N, and CLK2 generates the N-1 clock pulses, which is then fed to the FSM to change the state of the port. Which changed the states of the ports through the multiplexer, and all four ports write/read the data to/from the SRAM macro. Also, at each transition of the CLKP, the states were initialized to the highest priority port. Table II compares the proposed work with other published work. Here, the main advantage of the proposed design is that it uses an efficient 6T SRAM cell, while other work uses a higher number of transistor-based memory cells. This adds to the huge area overhead, while the area overhead of the proposed wrapper is very minimal. Another advantage of the proposed work is that all ports can be configured for both read and write operations, while in other works, the ports were fixed for either read or write operations. The overall architecture works at the clock frequency of 250MHZ, while the memory access frequency becomes 4×, i.e., 1GHz at 1.2V supply.

IV. CONCLUSION

This paper introduces an ultra-high-density multi-port SRAM architecture, achieved by designing a wrapper over a single-port SRAM. However, the same architecture can be scaled for any other SRAM bitcells. This wrapper circuit adds minimal area overhead compared to the significant increase resulting from modifying the memory bitcell, which typically accounts for about 60% of the overall macro area in larger SRAM macros. The proposed circuit was implemented using 65nm CMOS technology and validated with a 1.2V supply. The wrapper retains all features of the single-port design while taking up minimal space. It allows the SRAM macro to be configured with 1-port, 2-port, 3-port, or 4-port memory, with each port flexible for use as either read or write.

REFERENCES

- [1] H. Noguchi, S. Okumura, Y. Iguchi, H. Fujiwara, Y. Morita, K. Nii, H. Kawaguchi, and M. Yoshimoto, "Which is the best dual-port sram in 45-nm process technology?—8t, 10t single end, and 10t differential—," in 2008 IEEE International Conference on Integrated Circuit Design and Technology and Tutorial. IEEE, 2008, pp. 55–58.
- [2] N. S. Dhakad, E. Chittora, V. Sharma, and S. K. Vishvakarma, "R-inmac: 10t sram based reconfigurable and efficient in-memory advance computation for edge devices," *Analog Integrated Circuits and Signal Processing*, vol. 116, no. 3, pp. 161–184, 2023.
- [3] A. Ghosh, U. Bhattacharya, M. Kumar, and S. Banerjee, "Compiler compatible 5.66 mb/mm2 8t 1r1w register file in 14 nm finfet technology," *Integration*, vol. 70, pp. 126–137, 2020.
- [4] N. E. C. Akkaya, G. Chan, H. Liao, Y. Wang, and J. Chang, "A 135.6 tbps/w 2r2w sram with 12t logic bit-cell with vmin down to 335mv targeted for machine-learning applications in 6nm finfet cmos technology," in 2022 IEEE Symposium on VLSI Technology and Circuits (VLSI Technology and Circuits). IEEE, 2022, pp. 110–111.
- [5] R. Ohara, M. Kabuto, M. Taichi, A. Fukunaga, Y. Yasuda, R. Hamabe, S. Izumi, and H. Kawaguchi, "A 1w/8r 20t sram codebook for deep learning processors to reduce main memory bandwidth," *IEICE Techni*cal Report; *IEICE Tech. Rep.*, vol. 123, no. 144, pp. 41–44, 2023.
- [6] S.-F. Hsiao and P.-C. Wu, "Design of low-leakage multi-port sram for register file in graphics processing unit," in 2014 IEEE International Symposium on Circuits and Systems (ISCAS). IEEE, 2014, pp. 2181– 2184
- [7] S. Ataei, M. Gaalswyk, and J. E. Stine, "A high performance multi-port sram for low voltage shared memory systems in 32 nm cmos," in 2017 IEEE 60th International Midwest Symposium on Circuits and Systems (MWSCAS). IEEE, 2017, pp. 1236–1239.
- [8] H. Nguyen, J. Jeong, F. Atallah, D. Yingling, and K. Bowman, "A 7-nm 6r6w register file with double-pumped read and write operations for high-bandwidth memory in machine learning and cpu processors," *IEEE Solid-State Circuits Letters*, vol. 1, no. 12, pp. 225–228, 2018.
- [9] K. Sethi, "Design space exploration of algorithmic multi-port memories in high-performance application-specific accelerators," arXiv preprint arXiv:2007.09363, 2020.
- [10] H. Jain, M. Edwards, E. R. Elenberg, A. S. Rawat, and S. Vishwanath, "Achieving multi-port memory performance on single-port memory with coding techniques," in 2020 3rd International Conference on Information and Computer Technologies (ICICT). IEEE, 2020, pp. 366–375.
- [11] H.-M. Lam, F. Guo, H. Qiu, M. Zhang, H. Jiao, and S. Zhang, "Pseudo multi-port sram circuit for image processing in display drivers," *IEEE Transactions on Circuits and Systems for Video Technology*, vol. 31, no. 5, pp. 2056–2062, 2021.